

Functionalization of Chitosan Membranes through Phosphorylation: Atomic Force Microscopy, Wettability, and Cytotoxicity Studies

I. F. Amaral,^{1,2} P. L. Granja,¹ Luís V. Melo,³ B. Saramago,⁴ M. A. Barbosa^{1,2}

¹Laboratório de Biomateriais, Instituto de Engenharia Biomédica, Rua do Campo Alegre, 823, 4150-180 Porto, Portugal

²Departamento de Engenharia Metalúrgica e de Materiais, Faculdade de Engenharia, Universidade do Porto, Porto, Portugal

³Departamento de Física, Instituto Superior Técnico, Avenida Rovisco Pais, 1049-001, Lisboa, Portugal

⁴Centro de Química Estrutural, Instituto Superior Técnico, Avenida Rovisco Pais, 1049-001, Lisboa, Portugal

Received 20 September 2005; accepted 3 November 2005

DOI 10.1002/app.23737

Published online in Wiley InterScience (www.interscience.wiley.com).

ABSTRACT: Grafting negatively charged groups such as phosphates is a well-known strategy for inducing the deposition of apatite-like layers under simulated physiological conditions. In this investigation, chitosan was phosphorylated in an attempt to enhance its osteoconduction. Chitosan membranes were phosphorylated at 30°C with the H₃PO₄/Et₃PO₄/P₂O₅/butanol reaction system for periods up to 48 h. This method is an alternative to the phosphoric acid/urea/dimethylformamide phosphorylation method, which involves the use of much higher temperatures. In this study, the effects of the phosphorylation reaction time on the surface morphology and surface free energy of phosphorylated membranes were investigated with atomic force microscopy and static-contact-angle measurements, respectively. In addition, the modified membranes were evaluated with respect to their cytotoxicity toward bone cells through the

incubation of human osteoblastic cells with extracts of the materials for two different periods: 24 and 120 h. The results revealed a reduction of the average surface roughness at the nanometer scale with increasing phosphorylation reaction time. Wettability studies showed an increase in the polar component of the surface free energy with increasing reaction time as a result of the increase in the phosphate surface concentration. Cytotoxicity studies revealed no cytotoxic effect of phosphorylated membranes on osteoblastic cells, regardless of the incubation period. © 2006 Wiley Periodicals, Inc. *J Appl Polym Sci* 102: 276–284, 2006

Key words: atomic force microscopy (AFM); biocompatibility; biological applications of polymers; biomaterials; chitosan; polysaccharides

INTRODUCTION

Chitosan, a biodegradable polysaccharide usually obtained by the alkaline treatment of chitin, is a naturally occurring and renewable polysaccharide present in the exoskeletons of marine arthropods. With well-established biocompatibility, it is presently under investigation for a wide range of therapeutic applications, such as burn and wound dressings, sutures, bone fillers, engineered tissue scaffolds, and drug and gene delivery vehicles.^{1–3} Chitosan is a linear copolymer of glucosamine and *N*-acetyl glucosamine in a β 1→4 linkage, structurally similar to extracellular-matrix glycosaminoglycans. In chitosan, the molar frac-

tion of *N*-acetylated units is known as the degree of *N*-acetylation (DA), which, depending on the extent of deacetylation, can range from 0 to 50%. DA is a structural parameter affecting the charge density, solubility, and propensity to enzymatic degradation, with higher DAs leading to faster biodegradation rates.¹

Like most polysaccharides, chitosan has the ability to elicit specific cellular functions, namely as an immunoadjuvant (because of the ability of *N*-acetyl glucosamine residues to attract and activate polymorphonuclear leucocytes), inducing the production of cytokines and the subsequent regeneration of connective tissues.^{4–6} When applied to bone defects, chitosan and its derivatives enhance osteogenesis and angiogenic activity.^{7,8} In addition, because it can be readily processed into films and porous forms without the use of toxic solvents,⁹ an increasing number of chitosan-based scaffolds have been developed to be used as temporary templates for *in situ* bone regeneration and for cell-based bone therapies.^{10–12} Most often, chitosan is used in combination with calcium phosphates^{10,13} and growth factors¹⁴ or modified with cell-adhesive peptide motifs¹⁵ in an attempt to improve its mechan-

Correspondence to: I. F. Amaral (iamaral@ineb.up.pt).

Contract grant sponsor: Portuguese Foundation for Science and Technology; contract grant number: POCTI-FCB/41523/2001.

Contract grant sponsor: Portuguese Foundation for Science and Technology (to I.F.A. through Praxis XXI).

ical properties, osteoconduction, and ability to induce bone regeneration.

The response of osteoblasts and bone marrow stromal cells (BMSCs) to chitosan films is a matter of research interest. Osteoblast adhesion to chitosan films is dependent on the DA, lower DAs favoring cell adhesion,¹⁶ as reported for other anchorage-dependent cells.¹⁷ The cell adhesion of BMSCs to chitosan films follows the same trend: it is poor even for a DA as low as 4%, and osteogenic differentiation is attained only on films with a DA of 4%.¹² However, as both enzymatic degradation and chitosan biological aptitude to enhance tissue regeneration are dependent on the DA,¹⁸ the use of such low DAs may not always be desirable. As a result, alternative strategies to promote bone-cell adhesion and differentiation on chitosan have to be sought.

In polymeric implants used in orthopedics, the presence of a calcium phosphate overlayer is often desirable to promote osteoconduction and to ensure bone bonding. Grafting negatively charged functionalities, such as phosphates, is a well-known strategy for inducing the deposition of apatite-like layers under simulated physiological conditions.^{19–22} Recently, we applied this approach to chitosan membranes, using the $H_3PO_4/Et_3PO_4/P_2O_5$ /butanol phosphorylation reaction system, at 30°C, for periods up to 48 h.²³ The phosphate content increased with the reaction time, as shown by X-ray photoelectron spectroscopy (XPS) and attenuated total reflection/Fourier transform infrared, an atomic ratio of 0.73 P/N being obtained after 48 h of treatment. The latter was correlated to the degree of substitution at the surface, given that one nitrogen atom is present in each chitosan monomeric unit. The subsequent immersion of phosphorylated membranes [phosphorylated chitosan (P-chitosan)] in a $Ca(OH)_2$ solution, followed by incubation in a simulated plasma solution, resulted in the deposition of a multilayered and poorly crystalline porous mineral structure similar to bone mineral in terms of composition.²⁴

The phosphorylation method is based on the $H_3PO_4/Et_3PO_4/P_2O_5$ /hexanol reaction route optimized by Granja et al.²⁵ for the synthesis of highly phosphorylated cellulose derivatives and originally proposed by Touey and Kingsport²⁶ in 1956 for the synthesis of water-soluble and nondegraded cellulose phosphates. This method has the advantage of being carried out at room temperature, with low degradation of the polymer thus resulting. Additionally, upon implantation in rabbit bone defects, phosphorylated cellulose hydrogels induced no inflammatory response and showed osteointegration in the surrounding tissue.²⁷ The $H_3PO_4/Et_3PO_4/P_2O_5$ /butanol method is an alternative to the H_3PO_4 /urea/dimethylformamide method described for the phosphorylation of chitin and chitosan,^{28,29} which is the phosphorylation pathway usually followed to introduce phosphate

TABLE I
Chitosan Characterization in Terms of DA, M_w , M_n , and PDI

DA (%)	$M_w \times 10^5$	$M_n \times 10^5$	PDI
29.8 ± 1.21	5.4 ± 0.3	1.3 ± 0.2	3.9 ± 0.6

The listed results are the averages plus or minus the standard deviations. Four independent measurements and eight measurements made for two independent samples were used for the determination of the DA value and the average molecular weights, respectively.

functionalities into chitin fibers and chitosan films/sponges and which involves the use of high temperatures, typically higher than 120°C.^{21,30–32}

In this study, chitosan membranes phosphorylated for periods up to 48 h were characterized in terms of the surface morphology and surface free energy, which, together with the surface chemistry, constitute the main determinant features affecting the initial osteoblast response at the cell–material interface directly, or indirectly, by influencing the adsorption of adhesive glycoproteins.³³ In addition, P-chitosan was evaluated in terms of its cytotoxicity; this constitutes the initial step in a sequenced program of tests for the assessment of biocompatibility.³⁴

EXPERIMENTAL

Materials

Squid pen chitosan (Chitosan 123) was kindly supplied by France Chitine (Orange, France). All the reagents were analytical-grade.

Purification and characterization of chitosan

Purified chitosan was prepared by the filtration of a chitosan acid solution and subsequent alkali precipitation. The physicochemical characterization of the regenerated chitosan in terms of the DA and average molecular weights is shown in Table I. The DA was determined with infrared spectroscopy (System 2000 NIR FT-Raman spectrometer, Norwalk, CT) in KBr pellets, with the amide III band at 1320 cm^{-1} as the analytical band and the band at 1420 cm^{-1} as the internal reference band according to Brugnerotto et al.³⁵ The weight-average molecular weight (M_w) and number-average molecular weight (M_n) as well as the polydispersity index (PDI) were assessed by high-performance size exclusion chromatography with the 0.2M CH_3COONa /0.5M CH_3COOH system as the mobile phase according to Terbojevich et al.³⁶

Preparation of the chitosan membranes

Chitosan membranes were obtained via solvent casting from 1% (w/v) chitosan solutions in 1% (v/v)

acetic acid. After complete dissolution, the resulting gel was filtered, kept under reduced pressure to clear all the entrapped gas bubbles, and poured into $120 \times 120 \text{ mm}^2$ polystyrene Petri dishes (60 g/plate). After solvent evaporation, the resulting membranes were deprotonated in 0.5M aqueous NaOH and thoroughly washed with distilled and deionized water (DDW). Finally, they were cut into $30 \times 60 \text{ mm}^2$ strips and kept in absolute ethanol before chemical modification. For characterization, the chitosan membranes were dried at 30°C for 24 h in a vacuum oven and stored in a desiccator until further analysis.

Phosphorylation of the chitosan membranes

Surface phosphorylation was performed with the $\text{H}_3\text{PO}_4/\text{Et}_3\text{PO}_4/\text{P}_2\text{O}_5$ /butanol reaction system.²³ Briefly, 1-g chitosan membrane strips were suspended in 40 mL of 2-butanol in a round-bottom flask. The reaction mixture was prepared by the addition of 43 mL of H_3PO_4 to 37 mL of Et_3PO_4 , followed by the dropwise addition of P_2O_5 , under constant stirring. The reaction proceeded under an atmosphere of N_2 at 30°C with constant stirring in a thermostated orbital shaker. The reaction was carried out for different periods up to 48 h. After the chemical treatment, the membranes were rinsed with ethanol and suspended twice in this solvent for 30 min. Finally, they were dialyzed against DDW for 24 h to remove free inorganic phosphate and used for the biological assays or dried as described previously for characterization.

Surface characterization

Atomic force microscopy (AFM) imaging and roughness analysis

A Dimension 3100 atomic force microscope, equipped with a Nanoscope IIIa controller and an Extender Electronics module for phase-lag detection (Digital Instruments, Santa Barbara, CA), was used for the analysis. Imaging was performed in the tapping mode with standard tapping-mode Si tips. The samples were mounted on a magnetic puck with double-sided tape and analyzed in ambient air at room temperature. The surface roughness was determined in two different scan ranges, $1 \times 1 \mu\text{m}^2$ and $400 \times 400 \text{ nm}^2$, with Digital Instruments roughness analysis software. The following roughness height parameters were calculated: the average roughness (R_a ; i.e., the arithmetic average of the deviations from the center x - y plane), the root mean square of the deviations from the center x - y plane (R_q), and the sum of the height of the maximum peak with the depth of the maximum valley (R_{max}). The center plane is a plane such that the volumes enclosed by the image surface above and below are equal.³⁷ Measurements were made in three ran-

domly chosen areas per sample type with at least two different samples.

XPS

Survey spectra and high-resolution spectra for the C1s, O1s, N1s, and P2p regions were obtained with a VG Scientific (United Kingdom) Escalab 200 A with Mg $K\alpha$ X-ray radiation as the excitation source. The emitted photoelectrons were analyzed at a 90° take-off angle from the horizontal surface plane. Elemental atomic percentages were calculated from the integrated intensities of the XPS peaks, with the atomic sensitivity factors of the instrument data system taken into account.

Surface free energy determination

Wettability studies were performed with a OCA 15 Plus video-based optical contact-angle-measurement device provided with an electronic syringe unit (Dataphysics Instruments GmbH, Filderstadt, Germany). DDW, with a conductivity lower than $1 \mu\text{S}/\text{cm}$, and diiodomethane (>99%; Sigma-Aldrich Chemie GmbH, Germany) were used. The surface tension of the liquids was determined by the pendent drop method. Drops of 24 or $1.8 \mu\text{L}$ were generated from the tip of 1.65- or 0.52-mm needles, respectively. The measurements were carried out at 25°C inside a thermostated environmental chamber previously saturated with a pool of the liquid sample. The liquid densities at 25°C were determined with a density meter (Anton Paar GmbH, Germany). The polar and dispersive components of the surface tension of the liquids at 25°C were estimated from the corresponding values at 20°C , which were obtained from the literature.³⁸ The estimation was based on the assumption that the ratio of the dispersive and polar components of the surface tension did not vary with the temperature.

The samples used for wettability studies were immediately analyzed after drying. The strips were cut into squares ($20 \times 20 \text{ mm}^2$), and nitrogen was used to eliminate eventual dust particles from the surface. The static contact angles were measured at 25°C by the sessile drop method, with droplets of $4 \mu\text{L}$ for water and $1 \mu\text{L}$ for diiodomethane. Because of the swelling nature of the membranes and the eventual reorientation of surface groups,³⁹ time-dependent measurements were taken for 300 s, and the experimental contact angles were extrapolated to time zero. At least 10 drops were made per sample type in at least three different samples. The contact angles, surface tensions, and surface free energies were calculated with SCA20 software (version 2.0, DataPhysics), with the drop profiles fitted to the Young-Laplace equation. The polar and dispersive contributions of the surface energies were calculated according to the method of Owens and Wendt.⁴⁰

Cytotoxicity evaluation

Unmodified chitosan and P-chitosan were tested for cytotoxicity according to ISO standards (10993-5, 1992)³⁴ with the extract method. The modified membranes assayed for cytotoxicity were the 8-h P-chitosan membranes because they had shown the ability to mineralize under simulated physiological conditions in a previous study.²⁴ Cytotoxicity was evaluated by the measurement of the cell viability after cell incubation with the material's extracts for two different periods, namely 24 and 120 h. The longer period was used to study the effect of leachable products on cell proliferation.

Cell culture

MG-63 osteoblast-like cells from human osteosarcoma were obtained from the American Type Culture Collection and routinely cultured in α -minimal essential medium (α -MEM) supplemented with 10% (v/v) fetal bovine serum (FBS), 50 μ g/mL gentamicin sulfate, and 2.5 μ g/mL amphotericin B (all from Gibco/Invitrogen, Paisley, UK). Cultures were maintained in a humidified incubator at 37°C with 5% CO₂. When cells reached confluence, they were trypsinized and stained with trypan blue, and those that excluded the dye were counted with a hemocytometer. Cells were seeded at a density of 10⁴ viable cells/cm² in 96-well tissue culture polystyrene plates and incubated under the same conditions. The 24-h assay was performed when a subconfluent monolayer was obtained. The medium was then removed and replaced by the extracts. For the 120-h assay, the medium was removed and replaced by the extracts after a 4-h incubation period.

Extract preparation

Chitosan and 8-h P-chitosan membranes were used after sterilization in 70% ethanol for 30 min. The acidic groups of P-chitosan were neutralized by immersion in 20 mM NaOH for 60 min, rinsed twice in DDW, and then equilibrated in α -MEM for 60 min, the medium being exchanged every 15 min. The extracts were prepared by the incubation of the membranes in α -MEM (5 cm²/mL) supplemented with 50 μ g/mL gentamicin sulfate and 2.5 μ g/mL amphotericin B in an orbital incubator at 37°C for 120 h at 100 rpm. A sample of the extract vehicle subjected to the same extraction conditions was used as a control. At the end of this period, the membranes were removed, and the so-called extracts were obtained. Before being used, the extracts were serially diluted in a culture medium used as a control, supplemented with 10% (v/v) FBS, and sterilized by filtration (0.22 μ m). A fresh culture medium was used as a negative control, whereas a solution of

phenol prepared in a fresh culture medium (64 g/L) was used as a positive control.

Cell viability evaluation

At the end of each culture period, the number of viable cells was estimated with the 3-(4,5-dimethylthiazol-2-yl)-2,5-diphenyl tetrazolium bromide (MTT) assay. The MTT assay is a colorimetric method of determining cell viability based on the reduction of the yellow tetrazolium salt to insoluble blue formazan crystals by mitochondrial enzymes in viable cells.^{41,42} Given that the amount of formazan generated is directly proportional to the cell metabolic activity, the correspondent absorbance at 540 nm allows an estimation of the number of viable cells.⁴² Briefly, at the end of the incubation period, the extracts were removed, and the cell layers were rinsed with phosphate-buffered saline. Cells were then incubated with MTT (0.5 mg/mL in Dulbecco's medium without phenol red) at 37°C for 4 h. At the end of this period, the supernatant was discarded, and 100 μ L of dimethyl sulfoxide was added to dissolve the formazan crystals. After complete dissolution, the optical density of the supernatant was read at 540 nm with reference to 620 nm with a microplate spectrophotometer (SLT Labs Instruments GmbH, Salzburg, Austria). Both assays were repeated three times. The reported values are the average of eight replicates and are expressed as a percentage of the negative control.

Statistical analysis

The data were analyzed with the nonparametric Mann-Whitney U test, two-tailed asymptotic significance levels being considered. The results were considered statistically significant at $p \leq 0.05$. The Pearson correlation coefficient was used to determine the linear association between two variables. Calculations were performed with SPSS software for Windows (version 12.0).

RESULTS AND DISCUSSION

Surface characterization

AFM imaging and roughness analysis

Three-dimensional AFM images of unmodified and 48-h P-chitosan membranes, taken in a scan range of 1 \times 1 μ m² are shown in Figure 1. The chitosan membranes revealed a predominantly hill-valley-structured surface of nanoscale topography [Fig. 1(a)] in accordance with other reports.⁴³ The phosphorylated samples presented similar surface morphology, regardless of the reaction time [Fig. 1(b)].

The results concerning the roughness analysis are shown in Table II and correspond to a 1 \times 1 μ m²

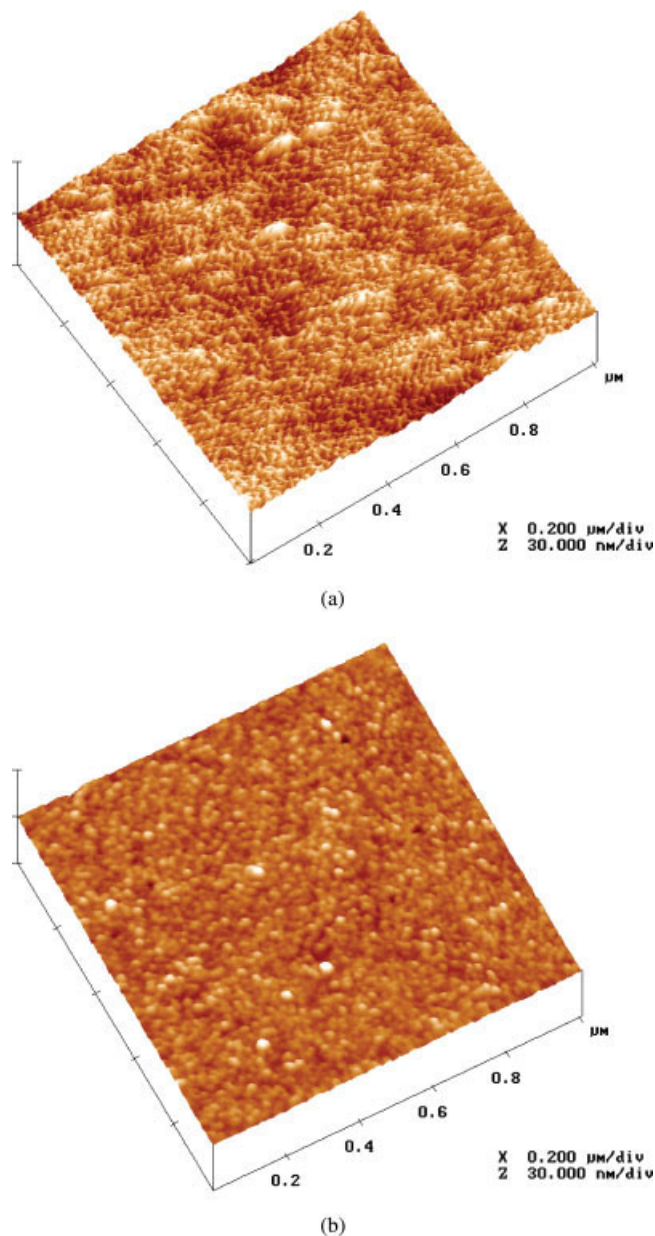


Figure 1 Tapping-mode three-dimensional AFM images of sample surfaces: (a) a chitosan membrane and (b) a 48-h P-chitosan membrane. The data were collected in a scan range of $1 \times 1 \mu\text{m}^2$ under ambient conditions. [Color figure can be viewed in the online issue, which is available at www.interscience.wiley.com.]

scanned area. Unmodified chitosan membranes revealed R_a values of 1.50 and 1.27 nm for scanned areas of $1 \times 1 \mu\text{m}^2$ and $400 \times 400 \text{ nm}^2$, respectively, indicating roughness at the nanometer scale. The maximum peak-to-valley differences determined in each of those measured areas were 17.5 and 12.1 nm, respectively, and they corresponded to the larger features imaged. The analysis of the substrates in different scan ranges resulted in different roughness values, higher values being found when larger areas were scanned.

This fact is frequently described because R_a is the arithmetic average of the deviations from the center x - y plane, as previously defined, and therefore is a function of the scan size.^{44,45} The phosphorylated samples presented lower R_a values than untreated membranes, although statistically significant differences were not found for all groups. However, a Pearson correlation coefficient of -0.802 was found between the phosphorylation reaction time and R_a , significant at the 0.001 level, suggesting that phosphorylation contributed to the smoothing of the membranes. The R_a data collected from a $400 \times 400 \text{ nm}^2$ scanned area showed a similar trend with the reaction time. Both chitin and chitosan are susceptible to acid hydrolysis, although chitosan is more resistant because of the protective effect of the protonated amine groups, which shield the glycosidic oxygen from protonation and, consequently, from hydrolysis.⁴⁶ The smoothing of chitosan membranes during chemical modification may thus be related to the acidic nature of this reaction medium.

XPS

The survey spectra of unmodified chitosan membranes confirmed the presence of carbon, oxygen, and nitrogen. XPS results showed an increase in the surface phosphorus concentration with the phosphorylation reaction time, a maximum of 4.7 atom % P being reached after 48 h of treatment, in agreement with previous results (Table III).²³

Surface free energy determination

The calculated surface tensions of water and diiodomethane were $71.5 \pm 0.1 \text{ mJ/m}^2$ and $50.5 \pm 0.1 \text{ mJ/m}^2$, respectively. The values found at 25°C were lower than the values reported in the literature for the same liquids at 20°C , as expected. The surface tension of most liquids decreases almost linearly with increasing temperature if the temperature is far below the boiling point of the liquid.³⁸

The contact-angle values determined for both unmodified chitosan and P-chitosan, as a function of the reaction time, are shown in Figure 2. The chitosan membranes presented a high water contact angle ($\cong 87.2^\circ$) and a surface free energy of 35.4 mJ/m^2 , which was entirely dominated by the dispersive component (Table III). Tomihata and Ikada¹ reported considerably lower water contact-angle values ($\cong 58^\circ$) for chitosan films prepared from chitosan with a similar DA (31%), although these results cannot be fairly compared because the latter regards the static-water-contact-angle measurements performed on water-swollen chitosan films. These results reveal that chitosan membranes have a hydrophobic solid-air interface, despite carrying polar functional groups, namely hydroxyl

TABLE II
Surface Roughness Parameters of Unmodified Chitosan and P-Chitosan as Functions of the Phosphorylation Reaction Time

Phosphorylation reaction time (h)	R_a (nm)	R_q (nm)	R_{max} (nm)
0	1.50 (1.25, 1.81)	2.01 (1.61, 2.60)	17.5 (13.1, 26.0)
1	1.14 (0.950, 1.33)	1.84 (1.39, 2.28)	24.8 (19.3, 30.4)
4	0.949 (0.896, 0.979) ^a	1.23 (1.17, 1.27) ^a	10.8 (9.64, 13.0) ^a
8	1.23 (1.15, 1.36)	1.58 (1.44, 2.28)	11.8 (11.0, 13.4)
12	0.894 (0.888, 0.902) ^a	1.10 (1.04, 1.13) ^a	8.89 (7.58, 9.88) ^a
24	0.833 (0.381, 1.11) ^a	1.17 (0.485, 1.63)	9.99 (3.99, 13.7)
48	0.345 (0.276, 0.388) ^a	0.446 (0.352, 0.501) ^a	5.49 (3.22, 7.82) ^a

The roughness was determined over a scanned area of $1 \times 1 \mu\text{m}^2$. The listed values are the averages of three measurements; the minima and maxima are shown in parentheses in that order.

^aStatistically significant difference in comparison with the unmodified chitosan membrane ($p \leq 0.05$).

and amine groups. Polymer surfaces are known to react to environmental changes to minimize their interfacial tension.³⁹ In an aqueous environment, the polar components tend to dominate, whereas in equilibrium with air or a vacuum, the nonpolar components (dispersive components) tend to dominate the interface.^{39,47} In this sense, the hydrophobic surface exhibited by chitosan membranes was probably a result of molecular reorientations that occurred during the vacuum-drying process.

Phosphorylation improved the wettability of the chitosan membranes, as expected. A water contact angle of 53.5° was obtained after 48 h of treatment. The change in the water contact angle was not attributed to surface physical heterogeneities because the chemical modification induced minimal changes in terms of the surface morphology, as shown by AFM roughness analyses. It is generally accepted that asperities in the range of $0.1\text{--}0.5 \mu\text{m}$ or below do not lead to significant hysteresis.^{39,48} Hence, the decrease in the water contact angle is mainly attributed to differences in the surface chemical composition, that is, to phosphate functionalities. The hydrophilicity of phosphate groups

is well established.^{20,49} Surfaces carrying phosphate functionalities have high affinity to polar liquids such as water because of the ionic nature of phosphate groups in an aqueous environment. On the other hand, the contact angles determined with diiodomethane as a testing liquid did not vary with the reaction time (Fig. 2). Diiodomethane, because of its apolar nature, is supposed to interact exclusively with the dispersive components of the solid. Because in this case only polar functionalities were introduced, the diiodomethane contact angle remained practically unaltered ($\cong 52^\circ$).

Concerning the surface free energy, the polar component of the surface free energy increased with the reaction time, leading to an increase in the total surface free energy from 35.42 to 51.58 mJ/m^2 as the membranes were reacted from 0 to 48 h, respectively (Table III). These results are in agreement with the presence of polar groups provided by phosphate functionalities. The plot of the polar component of the surface free energy versus the phosphorus surface concentration was fitted to a positive, exponential-like

TABLE III
Surface Free Energy (γ_{sv}) and Corresponding Dispersive (γ_{sv}^d) and Polar (γ_{sv}^p) Components of Unmodified Chitosan and P-Chitosan as Functions of the Phosphorylation Reaction Time

Reaction time (h)	Phosphorus (atom %) ²³	γ_{sv}^d (mJ/m^2)	γ_{sv}^p (mJ/m^2)	γ_{sv} (mJ/m^2)
0	0.00	93.3	6.7	35.4
1	1.06	90.9	9.1	37.2
4	2.31	88.4	11.6	38.3
8	2.87	84.1	15.9	39.0
12	2.96	82.4	17.6	40.1
24	3.42	74.3	25.7	44.6
48	4.71	64.3	35.7	51.6

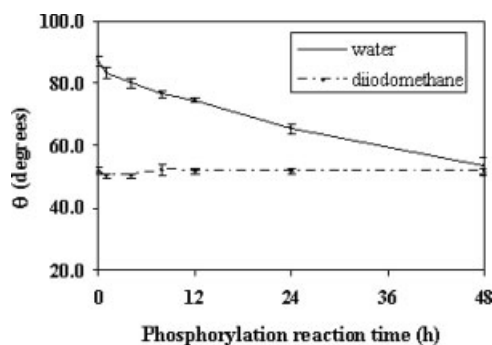


Figure 2 Static contact angle (θ) of water and diiodomethane on unmodified chitosan and P-chitosan as a function of the phosphorylation reaction time. The values represent the averages plus or minus the standard deviations ($n = 10$).

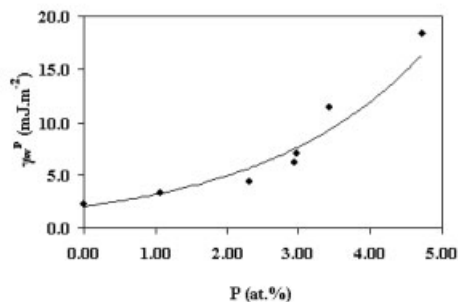


Figure 3 Polar component of the surface free energy (γ_{sv}^p) of unmodified chitosan and P-chitosan as a function of the phosphorus surface atomic percentage.

regression function (Fig. 3). The nonlinear increase of the polar component of the surface free energy is probably due to the reorientation of phosphate groups at the solid–air interface. During the vacuum-drying process, the hydrophilic phosphate groups are probably reoriented toward the inner part of the membranes to minimize the total surface free energy. As the phosphorus surface concentration increases, this reorientation may be partially hindered, leaving the phosphate groups more exposed and thus leading to the exponential increase of the polar component of the surface free energy. In comparison with XPS, contact-angle measurements are likely to be more sensitive to surface reorientation phenomena. Although the contact angle depends on the outermost surface molecular layers,³⁹ XPS data resulting from emitted photoelectrons analyzed at a 90° take-off angle use a thicker surface layer, typically about 10 nm.⁵⁰

In this study, the conventional technique of a sessile drop in air was used, and it required preliminary drying of the samples. An alternative would have been the use of immersion techniques for wettability studies, which allow the surface characterization of samples in the hydrated state. However, the measurement of the surface energy of water-containing polymers is problematic. The use of the captive air bubble or the inverted octane droplet techniques maintains the surface in a hydrated state but makes it difficult for the droplet to displace the adsorbed water layers. According to the work of Barnes et al.,⁵¹ the values of the surface free energy components determined in such a system are a function of both adsorbed and surface layers.

Cytotoxicity evaluation

24-h assay

No statistically significant differences were observed in the cell metabolic activity of MG-63 osteoblast-like cells cultured for 24 h in the presence of unmodified

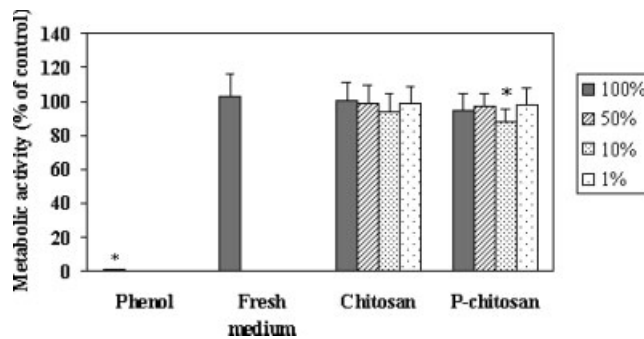


Figure 4 MG-63 osteoblast-like cell viability assessed by the MTT assay after 24 h of cell incubation with serially diluted extracts of chitosan membranes and 8-h P-chitosan membranes. Phenol (64 g/L) in a fresh culture medium and a fresh culture medium were used as positive and negative controls, respectively. The values are the averages plus or minus the standard deviations of eight cultures. The data come from one of three replicate experiments. The asterisks indicate a statistically significant difference from the control ($p \leq 0.01$).

chitosan or P-chitosan extracts in comparison with the control, independently of the dilution used (Fig. 4). When a 10% diluted P-chitosan extract was used, an exception occurred, resulting in an average relative metabolic activity of 87%. In addition, no correlation was found between the dilution of the extracts and the metabolic activity of the cells; this showed the absence of cytotoxic products released from the chitosan membranes subjected to this phosphorylation method.

120-h assay

Figure 5 shows the cell metabolic activity assessed after a 120-h period of cell incubation with the ex-

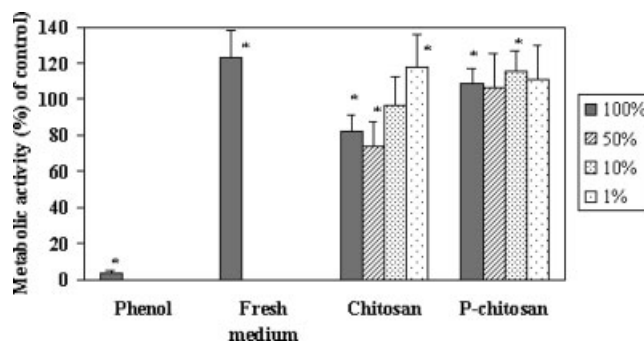


Figure 5 MG-63 osteoblast-like cell viability assessed by the MTT assay after 120 h of cell incubation with serially diluted extracts of chitosan membranes and 8-h P-chitosan membranes. Phenol (64 g/L) in a fresh culture medium and a fresh culture medium were used as positive and negative controls, respectively. The values are the averages plus or minus the standard deviations of eight cultures. The data come from one of three replicate experiments. The asterisks indicate a statistically significant difference from the control ($p \leq 0.01$).

tracts. A statistically significant decrease of the cell metabolic activity in the presence of an unmodified chitosan extract was observed and was particularly noticeable in the case of the less diluted extracts. In fact, a Pearson correlation coefficient of -0.76 , significant at the 0.001 level, was determined between the dilution of the extracts and the cell metabolic activity, indicating a linear dependence between these two variables. These results suggest a potential inhibitory effect of the chitosan extract on the number of viable cells at the end of the 120-h period and thus on cell proliferation. The inhibition of cell proliferation in the presence of the chitosan extracts was possibly related to the depletion of nutrients from the culture medium (α -MEM), which was promoted by the presence of positively charged amine functionalities from chitosan, which have the ability to ionically bind to negatively charged functional groups.^{52,53} When cells were cultured in the presence of extracts from P-chitosan, the aforementioned inhibitory effect on cell proliferation was not observed. Additionally, no correlation was found between the cell metabolic activity and the dilution of the extracts. It is possible that the presence of the negatively charged phosphate functionalities contributed to counterbalancing the positively charged amines from chitosan, leading to a less specific binding of elements from the culture medium.

According to other reports, both phosphorylated chitin and P-chitosan have shown *in vivo* biocompatibility when used as additives for calcium phosphate cements.^{54,55} Moreover, polyelectrolyte complexes containing phosphorylated chitin and P-chitosan have revealed no apparent cytotoxicity toward rat calvarial osteoblasts.⁵⁶ Our results revealed no cytotoxic effect of P-chitosan, in agreement with the previous studies.

CONCLUSIONS

The phosphorylation of chitosan membranes by the $H_3PO_4/Et_3PO_4/P_2O_5$ /butanol reaction system led to a reduction of the surface roughness with the reaction time at the nanometer scale, as shown by AFM studies, although the surface morphology of the membranes was not significantly altered. Wettability experiments clearly showed an increase in the polar component of the surface free energy with the reaction time and, as a result, in the total surface free energy. Cytotoxicity studies revealed no cytotoxic effect of P-chitosan membranes toward cultured bone cells, and this enables their use in further biological assays, such as the study of osteogenic differentiation of osteoprecursor cells on both phosphorylated and mineralized membranes.

The authors are grateful to France Chitine for the donation of squid chitosan.

References

- Tomihata, K.; Ikada, Y. *Biomaterials* 1997, 18, 567.
- VandeVord, P. J.; Matthew, H. W. T.; DeSilva, S. P.; Mayton, L.; Wu, B.; Wooley, P. H. *J Biomed Mater Res* 2002, 59, 585.
- Khor, E. *Chitin: Fulfilling a Biomaterials Promise*; Elsevier: Oxford, 2001.
- Peluso, G.; Petillo, O.; Ranieri, M.; Santin, M.; Ambrosio, L.; Calabro, D.; Avallone, B.; Balsamo, G. *Biomaterials* 1994, 15, 1215.
- Muzzarelli, R. A. A. *Cellul Mol Life Sci* 1997, 53, 131.
- Ishihara, M.; Nakanishi, K.; Ono, K.; Sato, M.; Kikuchi, M.; Saito, Y.; Yura, H.; Matsui, T.; Hattori, H.; Uenoyama, M.; Kurita, A. *Biomaterials* 2002, 23, 833.
- Muzzarelli, R. A. A.; Zucchini, C.; Ilari, P.; Pugnali, A.; Belmonte, M. M.; Biagini, G.; Castaldini, C. *Biomaterials* 1993, 14, 925.
- Muzzarelli, R. A. A.; Mattiolibellomonte, M.; Tietz, C.; Biagini, R.; Ferioli, G.; Brunelli, M. A.; Fini, M.; Giardino, R.; Ilari, P.; Biagini, G. *Biomaterials* 1994, 15, 1075.
- Madhally, S. V.; Matthew, H. W. T. *Biomaterials* 1999, 20, 1133.
- Zhao, F.; Yin, Y. J.; Lu, W. W.; Leong, J. C.; Zhang, W. J.; Zhang, J. Y.; Zhang, M. F.; Yao, K. D. *Biomaterials* 2002, 23, 3227.
- Lahiji, A.; Sohrabi, A.; Hungerford, D. S.; Frondoza, C. G. *J Biomed Mater Res* 2000, 51, 586.
- Amaral, I. F.; Lamghari, M.; Sousa, S. R.; Sampaio, P.; Barbosa, M. A. *J Biomed Mater Res Part A* 2005, 75, 387.
- Muzzarelli, R. A. A.; Muzzarelli, C. In *Chitosan in Pharmacy and Chemistry*; Muzzarelli, R. A. A.; Muzzarelli, C., Eds.; Atec Edizioni: Grottammare, Italy 2002; p 233.
- Lee, J. Y.; Nam, S. H.; Im, S. Y.; Park, Y. J.; Lee, Y. M.; Seol, Y. J.; Chung, C. P.; Lee, S. J. *J Controlled Release* 2002, 78, 187.
- Ho, M. H.; Wang, D. M.; Hsieh, H. J.; Liu, H. C.; Hsien, T. Y.; Lai, J. Y.; Hou, L. T. *Biomaterials* 2005, 26, 3197.
- Amaral, I. F.; Cordeiro, A.; Sampaio, P.; Barbosa, M. A. *J Biomat Sci: Polym*, accepted.
- Chatelet, C.; Damour, O.; Domard, A. *Biomaterials* 2001, 22, 261.
- Hidaka, Y.; Ito, M.; Mori, K.; Yagasaki, H.; Kafrawy, A. H. *J Biomed Mater Res* 1999, 46, 418.
- Mucalo, M. R.; Yokogawa, Y.; Suzuki, T.; Kawamoto, Y.; Nagata, F.; Nishizawa, K. *J Mater Sci: Mater Med* 1995, 6, 658.
- Tanahashi, M.; Matsuda, T. *J Biomed Mater Res* 1997, 34, 305.
- Yokogawa, Y.; Reyes, J. P.; Mucalo, M. R.; Toriyama, M.; Kawamoto, Y.; Suzuki, T.; Nishizawa, K.; Nagata, F.; Kamayama, T. *J Mater Sci: Mater Med* 1997, 8, 407.
- Granja, P. L.; Barbosa, M. A.; Pouysegue, L.; De Jeso, B.; Rouais, F.; Baquey, C. *J Mater Sci* 2001, 36, 2163.
- Amaral, I. F.; Granja, P. L.; Barbosa, M. A. *J Biomater Sci Polym Ed* 2005, 16, 1575.
- Amaral, I. F.; Granja, P. L.; Barbosa, M. A. *Key Eng Mater* 2004, 254, 577.
- Granja, P. L.; Pouysegue, L.; Petraud, M.; De Jeso, B.; Baquey, C.; Barbosa, M. A. *J Appl Polym Sci* 2001, 82, 3341.
- Touey, G. P.; Kingsport, T. (to Eastman Kodak Co.). U.S. Pat. 2,759,924 (1956).
- Fricain, J. C.; Granja, P. L.; Barbosa, M. A.; de Jeso, B.; Barthe, N.; Baquey, C. *Biomaterials* 2002, 23, 971.
- Sakaguchi, T.; Horikoshi, T.; Nakajima, A. *Agric Biol Chem* 1981, 45, 2191.
- Sakairi, N.; Shirai, A.; Miyazaki, S.; Tashiro, H.; Tsuji, Y.; Kawahara, H.; Yoshida, T.; Nishi, N.; Tokura, S. *Kobunshi Ronbunshu* 1998, 55, 212.
- Lee, Y. M.; Shin, E. M. *J Membr Sci* 1991, 64, 145.
- Varma, H. K.; Yokogawa, Y.; Espinosa, F. F.; Kawamoto, Y.;

- Nishizawa, K.; Nagata, F.; Kameyama, T. *Biomaterials* 1999, 20, 879.
32. Yokogawa, Y.; Nishizawa, K.; Nagata, F.; Kamayama, T. In *Bioceramics*; Ohgushi, H.; Hastings, G. W.; Yoshikawa, T., Eds.; World Scientific: Singapore, 1999; p 129.
33. Anselme, K. *Biomaterials* 2000, 21, 667.
34. Northup, S. J.; Cammack, J. In *Handbook of Biomaterials Evaluation: Scientific, Technical, and Clinical Testing of Implant Materials*; Recum, A. F., Ed.; Taylor & Francis: Philadelphia, PA, 1999; p 325.
35. Brugnerotto, J.; Lizardi, J.; Goycoolea, F. M.; Arguelles-Monal, W.; Desbrieres, J.; Rinaudo, M. *Polymer* 2001, 42, 3569.
36. Terbojevich, M.; Cosani, A.; Muzzarelli, R. A. A. *Carbohydr Polym* 1996, 29, 63.
37. Grundke, K.; Bogumil, T.; Werner, C.; Janke, A.; Poschel, K.; Jacobasch, H. J. *Colloids Surf A* 1996, 116, 79.
38. Kerkeb, M. L.; Gonzalezcaballero, F.; Chibowski, E. *J Colloid Interface Sci* 1993, 159, 439.
39. Andrade, J. D.; Smith, L. M.; Gregonis, D. E. In *Surface and Interfacial Aspects of Biomedical Polymers*; Andrade, J. D., Ed.; Plenum: New York, 1985; p 249.
40. Owens, D. K.; Wendt, R. C. *J Appl Polym Sci* 1969, 13, 1741.
41. Berridge, M. V.; Tan, A. S.; McCoy, K. D.; Wang, R. *Biochemica* 1996, 4, 14.
42. Mosmann, T. *J Immunol Methods* 1983, 65, 55.
43. Huang, R. Y. M.; Moon, G. Y.; Pal, R. *J Membr Sci* 2001, 184, 1.
44. Domke, J.; Dannohl, S.; Parak, W. J.; Muller, O.; Aicher, W. K.; Radmacher, M. *Colloids Surf B* 2000, 19, 367.
45. MacDonald, D. E.; Markovic, B.; Allen, M.; Somasundaran, P.; Boskey, A. L. *J Biomed Mater Res* 1998, 41, 120.
46. Roberts, G. A. F. *Chitin Chemistry*; Macmillan: London, 1992; p 350.
47. Andrade, J. D. *Clin Mater* 1992, 11, 19.
48. Wu, S. *Polymer Interface and Adhesion*; Marcel Dekker: New York, 1982.
49. Granja, P. L.; Pouysegu, L.; Deffieux, D.; Daude, G.; De Jeso, B.; Labrugere, C.; Baquey, C.; Barbosa, M. A. *J Appl Polym Sci* 2001, 82, 3354.
50. Ratner, B. D.; Caster, D. G. In *Surface Analysis—The Principal Techniques*; Vickerman, J. C., Ed.; Wiley: Chichester, England, 1997; p 43.
51. Barnes, A.; Corkhill, P. H.; Tighe, B. J. *Polymer* 1988, 29, 2191.
52. Domard, A. In *Advances in Chitin Science*; Domard, A.; Roberts, G.; Vårum, K., Eds.; Jacques André: Lyon, France, 1997; p 410.
53. Denuziere, A.; Ferrier, D.; Damour, O.; Domard, A. *Biomaterials* 1998, 19, 1275.
54. Wang, X. H.; Ma, J. B.; Feng, Q. L.; Cui, F. Z. *Biomaterials* 2002, 23, 4591.
55. Wang, X. H.; Ma, J. B.; Wang, Y. N.; He, B. L. *Biomaterials* 2002, 23, 4167.
56. Hamano, T.; Chiba, D.; Nakatsuka, K.; Nagahata, M.; Teramoto, A.; Kondo, Y.; Hachimori, A.; Abe, K. *Polym Adv Technol* 2002, 13, 46.